PERFORMANCE OF T-SHAPED DIAPHRAGM WALL IN A LARGE SCALE EXCAVATION

Hsii-Sheng Hsieh [1], Li-Hua Wu [2], Ting-Mei Lin [3], Jih-Cherng Cherng [4], and Wei-Ting Hsu [5]

ABSTRACT

Routine deep excavation projects require the use of retaining wall in conjunction with supports either in the form of internal bracings or tie-backs to resist lateral earth pressure. This paper presents a case in which a *T*-shaped diaphragm wall is used in lieu of internal bracings or tie-backs for a 9.6 m deep excavation in sandy soil. The *T*-shaped diaphragm wall has a relatively high rigidity that can withstand lateral earth pressure without excessive wall movement, which is a design advantage when there are existing buildings near the construction site. As indicated by instrumentation readings, the observed lateral displacement of *T*-shaped diaphragm wall was less than 1.5 cm. Numerical analyses by a beam-on-elastic-foundation program indicated that high rigidity of the *T*-shaped diaphragm wall is not the only governing factor that leads to a less-than-expected wall displacement. Additional side frictions developed along buttress surfaces of the *T*-shaped wall is believed to help in significantly reducing wall displacement in this particular case.

Key words: Deep excavation, *T*-shaped diaphragm wall.

1. INTRODUCTION

Most deep excavation projects in urban area use certain form of retaining wall together with lateral support system for earth retaining purpose. A wide range of retaining walls, such as soldier pile wall, sheet pile wall or diaphragm wall, can be selected pending on the ground condition and the required excavation depth. Lateral support system, which can either be tie-back anchors or internal bracings, is used to resist the active earth pressure exerting on the retaining wall for bottom-up excavations. As for top-down excavations, basement floors are utilized as lateral support.

Internal bracing system that consists of *H*-section steels in a crisscross layout is often the design choice for most deep excavation projects in Taiwan urban area. This type of lateral support system is very effective for small or mid-size excavations to control excavation induced movements, provided that the *H*-section steels are properly installed and preloaded. However, in case that the construction site is large in plan dimensions, the installation of an effective internal bracing system becomes a cumbersome task. Tie-back system is an obvious alternative under such circumstance, but this system is rarely used in Taiwan mainly because anchors would inevitably extend beyond the property lines. Top-down construction that uses floor slabs as lateral supports is another choice, but it is obviously a less attractive alternative to the project owner as drilled shafts are needed as vertical supports of the basement floors.

This paper presents a large excavation case of which the client rejected the use of conventional lateral support systems based upon schedule and financial concerns. *T*-shaped diaphragm wall alone, which provides a high flexural stiffness to withstand the lateral earth pressure (Xanthakos 1994), was adopted in this case as the excavation retaining system. The excavation was successfully completed and deformation of *T*-shaped diaphragm wall was found to be much less than expected. It is the purpose of this paper to present the field performance of this *T*-shaped diaphragm wall. Parametric studies using a simple but intuitive beam-on-elastic foundation numerical code were also carried out in an effort to delineate the behavior of the *T*-shaped diaphragm wall.

2. PROJECT DESCRIPTION

The construction site that involved the use of *T*-shaped diaphragm wall is a large scale community development project located in southern Taiwan, which is about 1 kilometer away from Ping-Tung airport (Fig. 1). The developer intended to build a total of twenty-six 14-story high-rise apartments in a site that measures about 40000 m^2 (roughly 350 m in length and 114 m in width) in plan area. A stretch of 3-story low-rise buildings covers the entire eastern boundary of the construction site at close proximity as indicated in Fig. 2. To the north and south of the construction site are empty lots. Right next to western side is a newly built 20 m wide county route underlain by several major utility lines. This county route serves as the main entrance to the construction site.

Excavation depth of the basement is 9.6 m. The excavation design uses a cast in place slurry wall as the retaining wall, which is also the permanent structural wall of the basement. As required by the developer, excavation of the basement had to be on a fast track schedule that virtually ruled out the use of a cumbersome internal bracing system. Tie-back system is not a viable choice as

Manuscript received May 12, 2011; revised October 13, 2011; accepted October 13, 2011.

[1] Senior Engineer (corresponding author), Trinity Foundation and Engineering Consultants (TFEC), Co. Ltd., Taipei, Taiwan, R.O.C. (e-mail: drhsieh@tfec.com.tw).
[2] Manager, TFEC, Co. Ltd., Taipei, Taiwan, R.O.C (e-mail: johnwu@tfec.com.tw).
[3] Engineer, TFEC, Co. Ltd., Taipei, Taiwan, R.O.C. (e-mail: tinmay@tfec.com.tw).
[4] Engineer, TFEC, Co. Ltd., Taipei, Taiwan, R.O.C. (e-mail: torsa@tfec.com.tw).
[5] Engineer, TFEC, Co. Ltd., Taipei, Taiwan, R.O.C. (e-mail: hsu1224@gmail.com).

Fig. 1 Geographic location of the project site

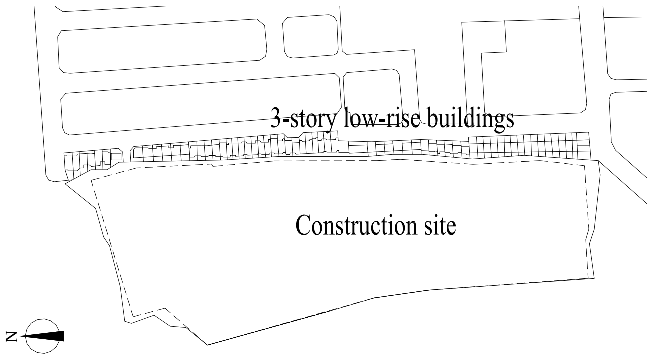

Fig. 2 Plan layout of the project site

the ground anchors would extend well beyond property line and provoke legal issues. Top-down scheme that uses basement floors as lateral supports was mentioned once, but was quickly rejected by the developer as this scheme would incur additional construction cost. Knowing that conventional excavation schemes would not meet the developer's requirements, the designer proposed to use *T*-shaped diaphragm wall that relies on its high flexural rigidity alone to support the 9.6 m deep excavation. This is a seemingly risky scheme at first glance since no lateral support of any kind was involved in the design. To the designer's surprise, the developer quickly agreed with the designer's unconventional scheme, perhaps the benefits of this excavation scheme significantly outweighed the possible risk. Of course the designer must make sure that the wall deformation is within tolerable limits if such an excavation scheme is to be adopted.

3. SOIL CONDITIONS

The project site locates in the heart of an alluvium plain. Site investigation reveals that subsurface of the project site consists a rather uniform layer of gray gravelly sand at least 50 m in thickness (Chang *et al*. 2001). The gravelly sand is a medium dense cohesionless material classified as SW-SM. Fine content of this SW-SM material is less than 20%, while the gravel content ranges from 15% ~ 30%. Visual inspection on the retrieved samples showed that the size of gravel is less than 25 mm. The SPT *N* values generally increase with depth. Most of the SPT *N* values are between 10 and 30. Test results on split spoon samples show that the natural water content of this gravelly sand is between 15% and 25%, and the average total unit weight is about 22 kN/m^3. The existence of gravels precluded the feasibility of retrieving undisturbed samples for shear strength tests, and the shear strength parameters were derived based upon engineering judgment. It is believed that the effective friction angle of this SW-SM material is somewhere between 31° and 35°. Uncertainty on the soil strength parameter was a lingering problem for the designer. The designer nonetheless had to make quick decisions to complete the excavation design.

Observation wells installed within the project site indicated that the groundwater table was fluctuating between 4.9 m and 5.4 m below ground surface. Slug tests were also carried out in several boreholes, revealing a more or less uniform permeability of 3×10^{-4} m/sec for this thick layer of gravelly sand.

4. EXCAVATION SCHEME

The excavation sequence for this large scale excavation is schematically shown in Fig. 3, which consists of the following stages:

Stage 1: Construct the *T*-shaped diaphragm wall.

Stage 2: Excavate central part of the basement to 9.6 m below surface.

Stage 3: Construct central part of the basement structure.

Stage 4: Extend floor slab of level-1 basement to the perimeter diaphragm wall.

Stage 5: Remove the berm and demolish buttress of the *T*-shaped wall.

Stage 6: Complete the remaining basement structure.

As shown in Fig. 3, a berm relatively small in size was left along with the *T*-shaped wall in the main excavation stage (Stage 2). This berm is 2 m wide on top and about 7 m wide at the bottom, slope of the berm is 45°. The contractor argued that the berm was too small to have any significant contribution on the overall stability of *T*-shaped wall, and proposed to eliminate the berm in the excavation design to expedite the construction of basement structure. The designer on the other hand insisted that the berm was essential to the retaining system, which must be left in place to provide added insurance to the large scale excavation. The developer then made the final decision that the berm was to stay for the peace of mind. In the field, slope of the berm was not stable, small scale slides on the surface of the slope were often observed.

Extending the floor slabs from the completed basement structure to the perimeter diaphragm wall provided additional lateral supports, which allowed the contractor to demolish buttresses of the *T*-shaped wall in latter construction stages. Superstructures of this project were all located at least one bay away from the perimeter diaphragm wall, therefore the construction of superstructures was not affected by stages 4 ~ 6 once central part of the basement structure was completed. This excavation scheme eliminated altogether the use of steel *H*-sections as internal bracings, and expedited the construction of superstructures. The developer's requirement of an inexpensive and efficient excavation scheme was therefore fulfilled.

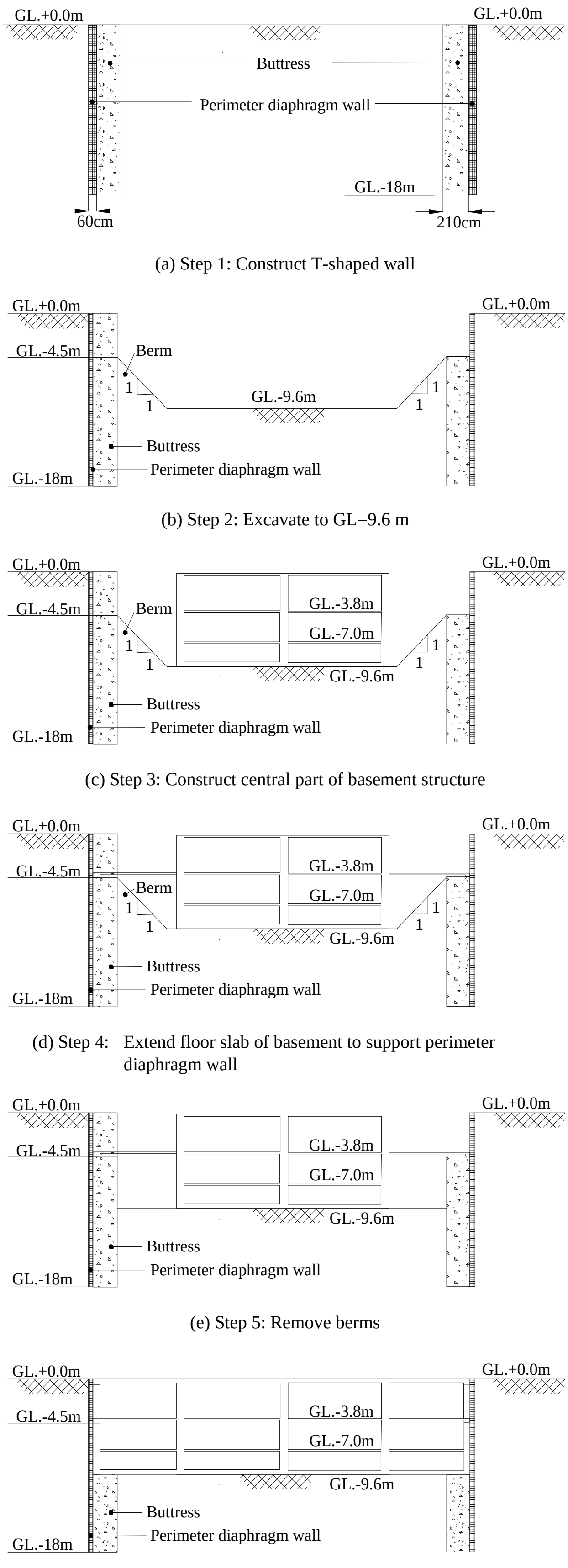

(a) Step 1: Construct T-shaped wall

(b) Step 2: Excavate to GL−9.6 m

(c) Step 3: Construct central part of basement structure

(d) Step 4: Extend floor slab of basement to support perimeter diaphragm wall

(e) Step 5: Remove berms

(f) Step 6: Demolish buttresses and complete basement structure

Fig. 3 Excavation sequence of the basement

It has to be pointed out that upper parts of buttress wall as shown on the left hand side of Fig. 3 were not demolished with excavation. The upper parts of buttress wall were purposely left in place to provide additional protection to the adjacent buildings until floor slab at ground level was completed.

5. LAYOUT AND DETAILS OF *T*-SHAPED DIAPHRAGM WALL

Layout and details of the *T*-shaped wall must be elaborated. Typical layout of the *T*-shaped diaphragm wall is shown in Fig. 4, which consists of perimeter wall and buttresses spaced at a distance of 9 m. The perimeter length of the project site is about 930 m, requiring the installation of about 90 buttresses together with the perimeter diaphragm wall. The perimeter wall and buttress walls are each 0.6 m in thickness and 18 m in depth. As for the construction of *T*-shaped diaphragm wall, primary panels with a typical length of 3 m were sandwiched between secondary panels with a typical length of 6 m. The secondary panels are *T*-shaped panels that were intentionally dredged to a T shape so the perimeter wall and buttress can be cast into one integral unit to achieve the designed performance of *T*-shaped wall. Special cares were needed to maintain the stability of *T*-shaped trenches, which appeared to be an easy task as reported by the diaphragm wall contractor. Worth mentioning is that the buttresses were not reinforced by rebars, which made the demolition of buttress walls a much easier task in the late stages of construction.

An overlapping type of joint was adopted to connect primary and secondary panels (Fig. 5). This type of overlapping joint is considered as a watertight structural joint capable of carrying moment and shear (Lee *et al*. 1992) when the diaphragm wall deforms. This is a feature essential to the overall performance of the *T*-shaped wall. The earth pressure and water pressure were acting on a continuous retaining wall rather than on individual panels.

6. DEWATERING SCHEME

Since the gravelly sand is highly permeable, it is expected that a large volume of ground water has to be pumped out to keep the construction site dry. Local practice usually requires that the ground water table within the construction site be maintained one meter below the excavation level. That is to say, the ground water has to be drawn down from the original level (GL.–5 m) to GL.−10.6 m, which is a net drawdown of about 5.5 m.

A group of local dewatering contractors were consulted about the possible pumping rate and possible layout of the deep wells. Since no contractor had dewatering experience with large scale project such as this one, they had diverse opinions about the possible pumping rate. Using a representative permeability of 3×10^{-4} m/sec for the thick layer of gravelly sand as a calculation basis, it was roughly estimated that a pumping rate of 20 cubic meters per minute (20 m^3/min) is needed to keep the ground water level at GL.–10.6m. A total of 200 deep wells were installed within the construction site. They were positioned near the perimeter diaphragm wall and spaced at 4 ~ 5 m intervals. Depth of the deep well is 18 m, and each well is equipped with a 7.5 HP submersible pump.

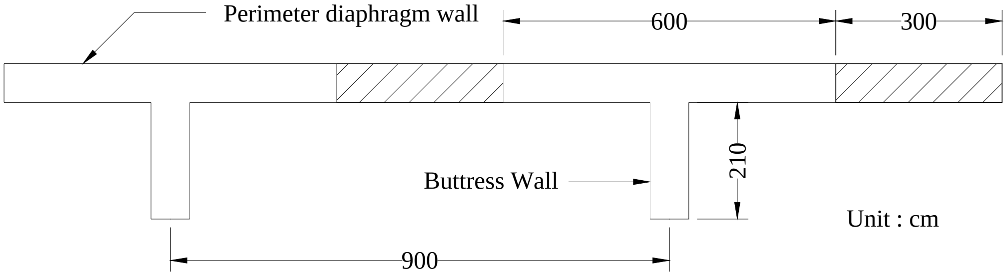

Fig. 4 Layout of the *T*-shaped wall

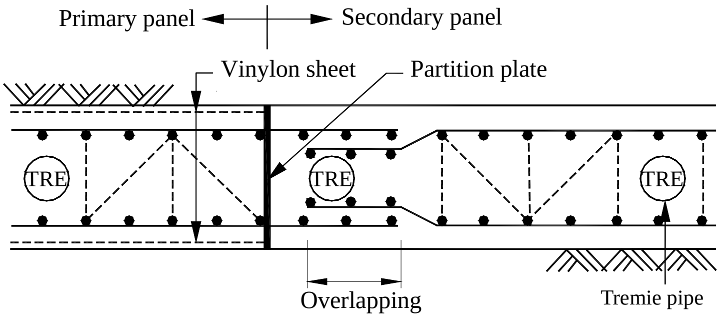

Fig. 5 Schematic diagram of the overlapping joint

In the early stage of excavation, the dewatering system was in full capacity, *i.e.*, all of the 200 deep wells were in operation. The discharge rate was found to decrease with time, allowing the dewatering contractor to shut down part of the deep wells. In the end of basement excavation, only 50 out of the 200 deep wells were in operation. It appeared that the dewatering system was over designed. Photos showing the layout and operation of deep wells are presented in Figs. 6 and 7.

Fig. 6 Deep wells installed near perimeter wall

Fig. 7 Deep wells in operation

7. POSSIBLE DISPLACEMENT OF *T*-SHAPED WALL

Though difficult to imagine, very limited time and budget were allocated for the excavation design. The designer was not able to thoroughly study the behavior of *T*-shaped wall for a large scale project like this. The only tool available to the designer at the design stage was a beam-on-elastic foundation computer code (RIDO 1991), which is a commercial code that treats soils as springs with limited capacities. The stiffness of soil spring is characterized by horizontal modulus of subgrade reaction (K_h), which is an empirical number roughly proportional to the SPT N value of the sandy soil. On the other hand, capacity of the soil spring cannot exceed passive resistance of the soil, which in turn, is a function of the effective friction angle of the sandy soil. This program was extensively used to assess the possible deformation of the *T*-shaped wall via a series of parametric studies.

7.1 Input Parameters

Among the RIDO input parameters, flexural stiffness of the *T*-shaped wall is the only parameter that can be accurately calculated. The *T*-shaped wall is modeled as a beam with an equivalent flexural stiffness. Friction angle of the gravelly sand is regarded as a variable ranging from 30° and 35°. Another important input parameter is the ground water level behind the *T*-shaped wall. The original ground water level was at about 5 m below surface, which could drop as a result of dewatering during the basement excavation stage. As a design requirement, ground water level within the project site must be lowered to 1 m below the final excavation depth (*i.e.*, GL.–10.6 m) to accommodate the construction of basement structure. Seepage underneath the 18 m deep diaphragm wall is likely to occur owing to the high permeability of the gravelly sand. But how much the ground water level would drop as a consequence of seepage is difficult to estimate. As suggested by experienced local dewatering contractor, a 2 m draw down is most likely to occur. To account for all possibilities, ground water levels were considered to vary from GL.–5 m to GL.−10.6 m in the RIDO analyses.

Surcharge loading acting on the ground surface of the retaining side had to be addressed too. Traffic, construction equipments, adjacent buildings, *etc*., are all likely sources of surcharge loading. Since there is a long stretch of 3-story reinforced concrete residential buildings at close proximity to the project site as indicated in Fig. 2, the maximum value of surcharge loading could reach up to 40 kPa. Surcharge loadings varied from 0 to 40 kPa were accounted for in the RIDO analyses. These surcharge loadings could dominate the behavior of *T*-shaped wall, which lacks of lateral supports and deform like a cantilever.

Input parameters are listed in Table 1, including flexural stiffness of the *T*-shaped wall, horizontal modulus of subgrade reaction (K_h) and effective friction angle of the gravelly sand, *etc*. The K_h value is usually taken as 200 N (t/m^3), where N is the typical SPT N value for a cohesionless layer. The average N value is taken as 15, therefore, K_h = 3000 t/m^3 = 29430 kN/m^3.

7.2 Possible Displacement of *T*-shaped Wall

As mentioned before, the designer was not sure about the exact value of the effective friction angle, nor the amount of drawdown. Parametric studies were carried out by varying the effective friction angles, ground water levels and surcharge loadings to examine all possible displacement curves of the *T*-shaped diaphragm wall. First, assuming the ground water level was at GL.–7 m on the retaining side, displacement of the *T*-shaped wall was estimated by varying the effective friction angle from 30° to 35°. Surcharge loadings ranging from 0 to 40 kPa were also incorporated in the parametric studies. As shown in Fig. 8, the displacement curves for a 40 kPa surcharge loading all exhibit a cantilever pattern which has a maximum value at top of the wall. This displacement pattern is typical for an unsupported retaining wall, and the main concern is obviously how much the wall moves at the top of the wall. If the maximum lateral movement at top of the wall is within an acceptable limit, then the performance of *T*-shaped wall is considered satisfactorily.

The other concern is the integrity of adjacent buildings with shallow footings situated right next to the project site. It is desirable that the maximum lateral displacement of *T*-shaped wall be kept within 2.54 cm (one inch) so that the induced settlement can also be limited to less than 2.54 cm (Woo and Moh 1990). It is a general belief that buildings with shallow footing can sustain a settlement of 2.54 cm without noticeable damage. If the contractor can keep the maximum lateral displacement of *T*-shaped wall within 2.54 cm, the adjacent buildings would have a better chance to survive the nearby excavation.

The maximum calculated values of wall displacement were presented in Table 2 and Fig. 9, which showed that the maximum wall displacement decreased with the increase of effective friction angle. The actual effective friction angle is likely to be 32°±1°, suggesting that the maximum wall displacement can be from 7.1 cm to 8.5 cm for a surcharge loading of 40 kPa.

Table 1 RIDO input parameters

(a) Soil parameters

Layer	Depth (m)	Soil Type	γ_t (kN/m^3)	c' (kPa)	ϕ' (°)	K_h (kN/m^3)
I	20	SM	20.6	0.0	30 ~ 35	29,430

(b) Diaphragm wall parameters

Type	Depth (m)	Thickness (m)	f_c' (kPa)	$E_c I$ (kN-m^2)
Perimeter diaphragm wall	18	0.6	20,000	186,390
T-shaped diaphragm wall	18	0.6	20,000	981,000

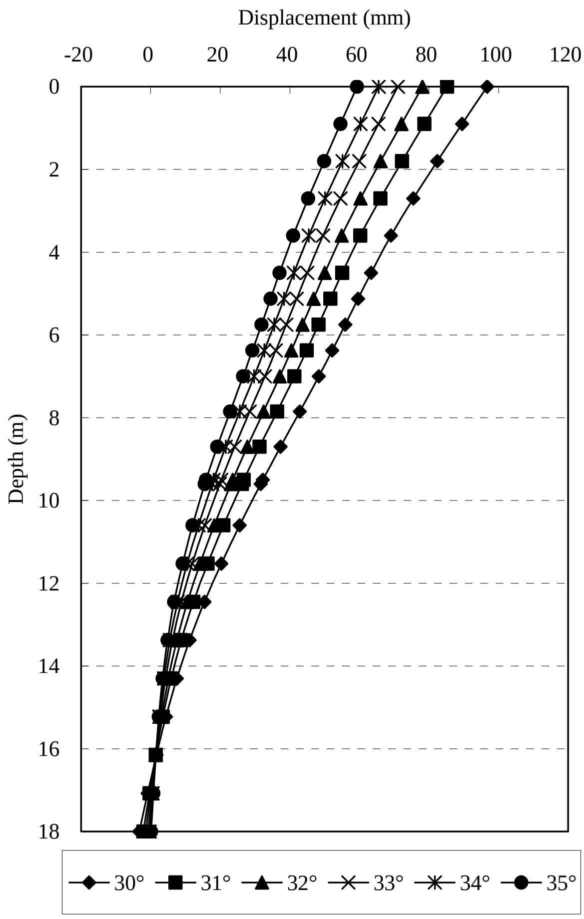

Fig. 8 Analytical displacement curves of the *T*-shaped wall (40 kPa surcharge loading and 2 m drawdown)

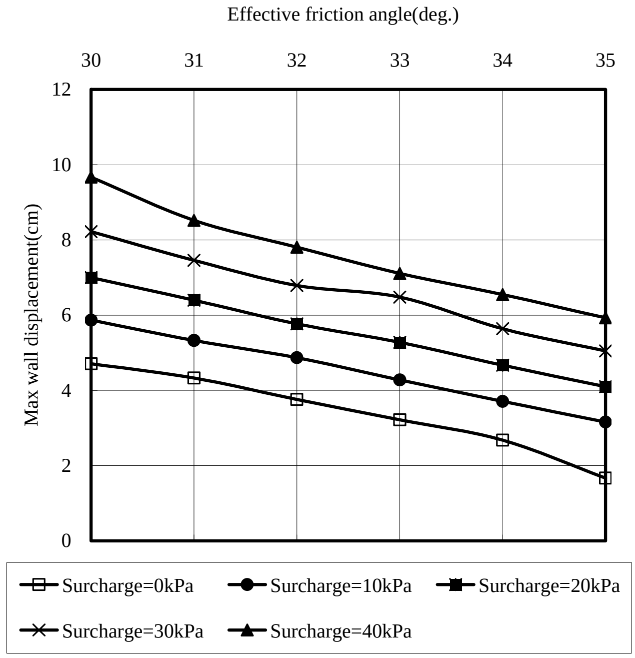

Fig. 9 Relationship between maximum wall displacement and effective friction angle (2 m drawdown, RIDO calculation)

Table 2 Maximum displacement of *T*-shaped wall (2m drawdown, RIDO calculation)

Max. displacement (cm) / Effective friction angle (°) / Surcharge(kPa)	30	31	32	33	34	35
0	4.71	4.33	3.76	3.22	2.68	1.67
10	5.87	5.33	4.87	4.28	3.71	3.16
20	7.00	6.40	5.77	5.28	4.67	4.10
30	8.22	7.46	6.79	6.48	5.64	5.05
40	9.67	8.52	7.81	7.11	6.55	5.93

The above calculations were based upon the assumption that the ground water level on the retaining side of *T*-shaped wall would drop from GL.–5 m to GL.–7 m as a result of dewatering within the project site. Further drop down of the ground water level would help in reducing the wall displacement to a lower value. The worst case scenario would be the ground water level on the retaining side of *T*-shaped wall remained unchanged at GL.–5 m during basement excavation, which meant the diaphragm wall served as a perfect cutoff. In that case, the *T*-shaped wall would displace at top for about 8.4 cm to 10.3 cm if the effective friction angle falls between 31° and 33°. The maximum calculated values of wall displacement for different ground water levels were presented in Table 3 and Fig. 10.

Berm that was left in place on the excavation side is essential to the stability of the *T*-shaped wall. As indicated in Table 4 and Fig. 11, the *T*-shaped wall could either fail or exhibit large lateral deformation in the absence of berm.

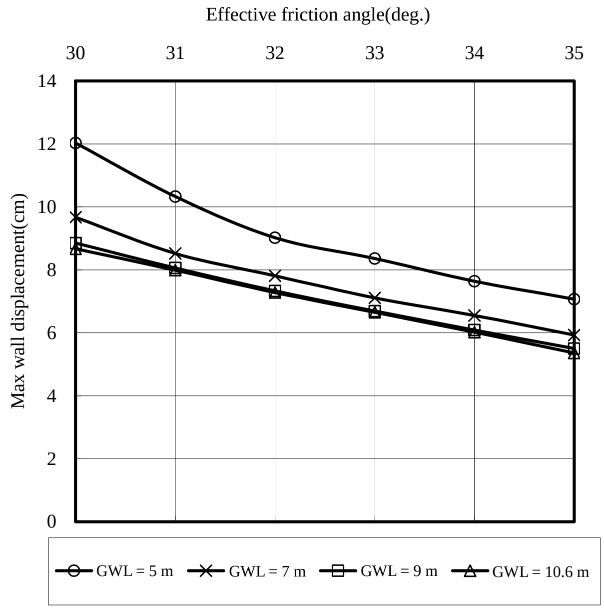

Fig. 10 Relationship between maximum wall displacement and effective friction angle (40 kPa surcharge loading, RIDO calculation)

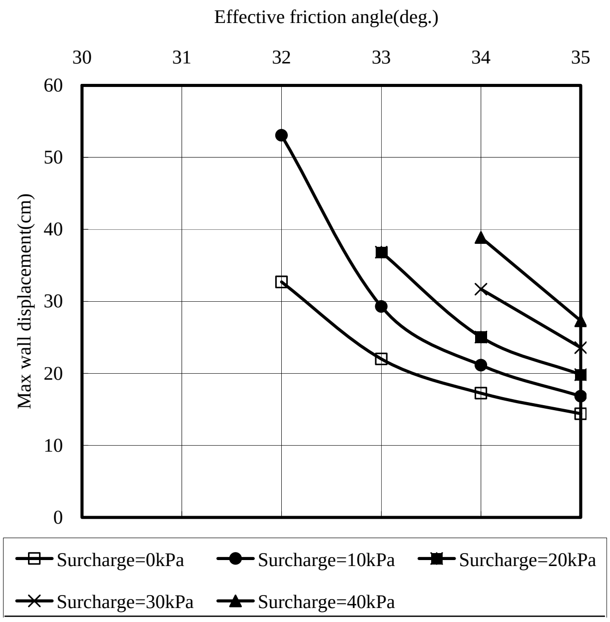

Fig. 11 Relationship between maximum wall displacement and effective friction angle (2 m drawdown, no berm, RIDO calculation)

Table 3 Maximum displacement of *T*-shaped wall (40 kPa surcharge loading, RIDO calculation)

Max. displacement (cm) / Effective friction angle (°) / Ground water depth (m)	30	31	32	33	34	35
− 5.0	12.03	10.33	9.02	8.36	7.64	7.07
− 7.0	9.67	8.52	7.81	7.11	6.55	5.93
− 9.0	8.85	8.06	7.33	6.69	6.09	5.50
−10.6	8.67	7.99	7.28	6.65	6.02	5.36

Table 4 Maximum displacement of *T*-shaped wall (2 m drawdown, no berm, RIDO calculation)

Max. displacement (cm) / Effective friction angle (°) / Surcharge(kPa)	30	31	32	33	34	35
0	Failure	Failure	32.69	22.01	17.24	14.40
10	Failure	Failure	53.05	29.29	21.14	16.83
20	Failure	Failure	Failure	36.83	25.04	19.82
30	Failure	Failure	Failure	Failure	31.69	23.57
40	Failure	Failure	Failure	Failure	38.88	27.31

7.3 Best Estimate on the Possible Displacement of *T*-shaped Wall

Amid all the uncertainties, the designer had to decide if the actual displacement of *T*-shaped wall is acceptable. Without the help of 3-D numerical analyses, the designer could only rely on the results of 1-D RIDO analysis as well as engineering judgment to reach a plausible conclusion. In order to do so, the designer must select appropriate parameters as RIDO input. The most important RIDO input is perhaps the effective friction angle of the gravelly sand, which is believed to fall between 31° and 33°, and a mid value of 32° appeared to be a reasonable choice as the design parameter. As for the ground water level behind *T*-shaped wall, local dewatering contractor's suggestion was adopted, who said the ground water level would drop at least 2 m below the original level, *i.e.*, at GL.–7 m after the excavation was completed. The representative surcharge loading was taken as 20 kPa, which was thought to be the average weight of adjacent buildings.

As indicated in Table 2, the maximum lateral displacement of the *T*-shaped wall is about 5.77 cm if the effective friction angle, surcharge loading and ground water level were taken as 32°, 20 kPa, and GL.–7 m, respectively. The developer was comfortable with this amount of wall displacement and accepted the *T*-shaped wall design. However, the designer was not so optimistic and urged the client to be prepared for the excessive ground settlement that could be detrimental to the adjacent buildings. Scheme to underpin the adjacent buildings might have to be undertaken if monitoring results in the early stage of excavation showed that the wall displacement and building settlement could be excessive.

In summary, the designer's best estimate is that the *T*-shaped wall should deform no more than 6 cm. The contingency plan is to underpin the adjacent buildings should wall deformation and building settlement exceed 6 cm and 2.5 cm, respectively.

8. FIELD PERFORMANCE OF *T*-SHAPED DIAPHRAGM WALL

The project site was lightly instrumented to monitor the wall displacement, ground water variation and settlement of adjacent buildings. Layout of the instrumentation system is shown in Fig. 12. Nine inclinometer casings (SI-1 ~ SI-9), each 18 m in depth, were installed within perimeter diaphragm wall to monitor excavation induced lateral displacements. Six out of the nine inclinometer casings were placed on the east side where adjacent buildings were located. For ease of installation, the inclinometer casings were generally located in secondary panels about 1 m away from the partition plate. Sixteen observation wells, each 12 m in depth, were installed around the project site to monitor the variation of groundwater level behind the *T*-shaped wall during excavation. Ninety-five settlement markers, together with seventeen tilt meters, were installed on the adjacent buildings. Optical survey techniques were used to measure building settlements. It is worth noting that the diaphragm walls were not anchored in non-yielding ground, the bottoms of walls could move inward or outward during basement excavation and could not be regarded as fixed reference points. To mitigate this problem, movements at tops of the inclinometer casings were independently measured by surveying from reference points.

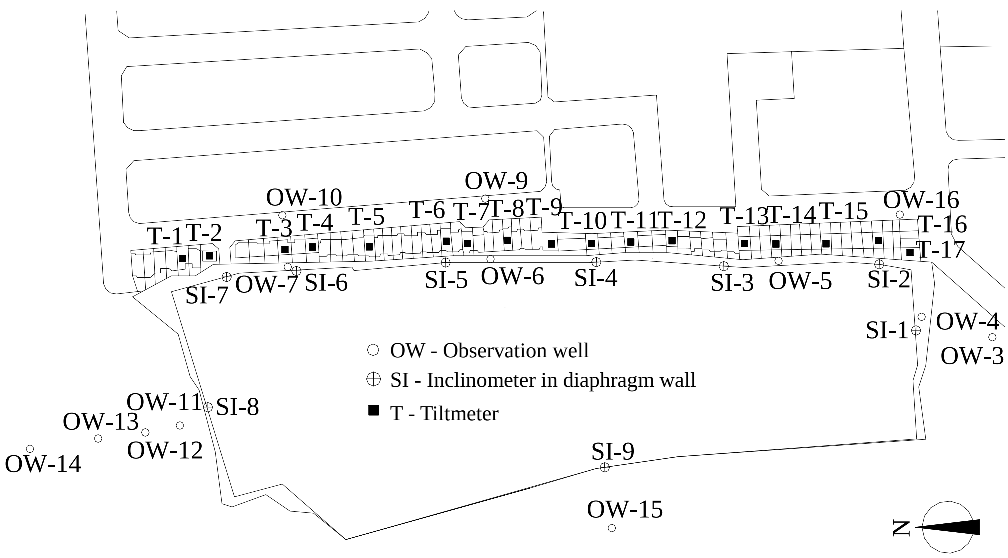

Fig. 12 Layout of instrumentation system

8.1 Observed Wall Displacement

Lateral movements of the diaphragm walls at the end of second excavation stage, which is considered the most critical stage, are presented in Fig. 13. The results indicate that the maximum lateral displacements of the diaphragm walls were less than 1.4 cm (0.15% of excavation depth), which occurred at top of the diaphragm wall. The pattern of displacement curves shown in Fig. 13 is typical of an unsupported cantilever. The relatively small displacement at top of the wall is a good indication that the *T*-shaped wall is in a stable condition. Flexural stiffness of the *T*-shaped wall and the developed passive resistance were capable of withstanding the pressure acting on the retaining side of the diaphragm wall. It is also worth mentioning that for a carefully conducted instrumentation program, the accuracy of inclinometer reading generally falls within 0.2 cm ~ 0.3 cm/30 m, which is about 12% of the maximum diaphragm wall displacement (1.4 cm/18 m) of this case.

In this case, the diaphragm wall served as the temporary and permanent excavation support wall. Buttresses of the *T*-shaped wall were removed after B1 and 1FL floors were completed. As a result, the lateral earth pressures were transferred to the more rigid basement floors. Inclinometer readings showed that the additional diaphragm wall displacement after construction stage 2 was insignificant. It is for this reason that the parametric analyses only focused on excavation stage 2, and the subsequent stages were not modeled.

8.2 Observed Building/Surface Settlement

A total of 59 settlement markers and 17 tiltmeters were mounted on the adjacent buildings. However, measurements on these settlement markers could not be carried out on a regular basis because of access problem. Sporadic data showed that settlement of the adjacent buildings was somewhere between 2 and 7 mm. The average tilting of surrounding buildings was less than 1/1200. Except that a few building owners complained about minor cracks on their partition walls, the adjacent buildings were otherwise in sound conditions.

There were 36 surface settlement markers installed around the construction site. Periodic measurements on these markers over a six-month period showed that surface settlements varied from 8 mm to 20 mm. Since surface settlement markers were more or less randomly deployed, it was not possible to construct the settlement profile behind the *T*-shaped wall. In general, settlement markers located near mid span of the construction site exhibited larger settlement.

In summary, no distinct patterns of building settlement or tilting were observed. It should be noted that the amount of settlement and tilting of adjacent buildings are not just governed by excavation and dewatering process. Nearby activities, such as dynamic traffic loading induced by heavy duty trucks, may have triggered slight movement of the adjacent buildings that in turn led to misleading readings.

8.3 Variation of Ground Water Level

Starting from the early stage of basement excavation, ground water levels were periodically monitored for a span of about 6 months until the basement structures were completed. As indicated by the monitoring results, ground water level around the construction site dropped steadily as a result of extensive dewatering within the project site, though occasional heavy rainfall could cause a temporary rise of the ground water level. Of all the 16 observation wells, the lowest and highest ground water levels ever recorded during basement excavation stage were listed in Table 5. In average, the high and low ground water levels were found to be at GL.–4.9 m and GL.–8.3 m, respectively. The average high ground water level can be regarded as the original water level before the commencement of basement excavation. The lowest ground water levels were generally observed at late stage of basement excavation, and the average low

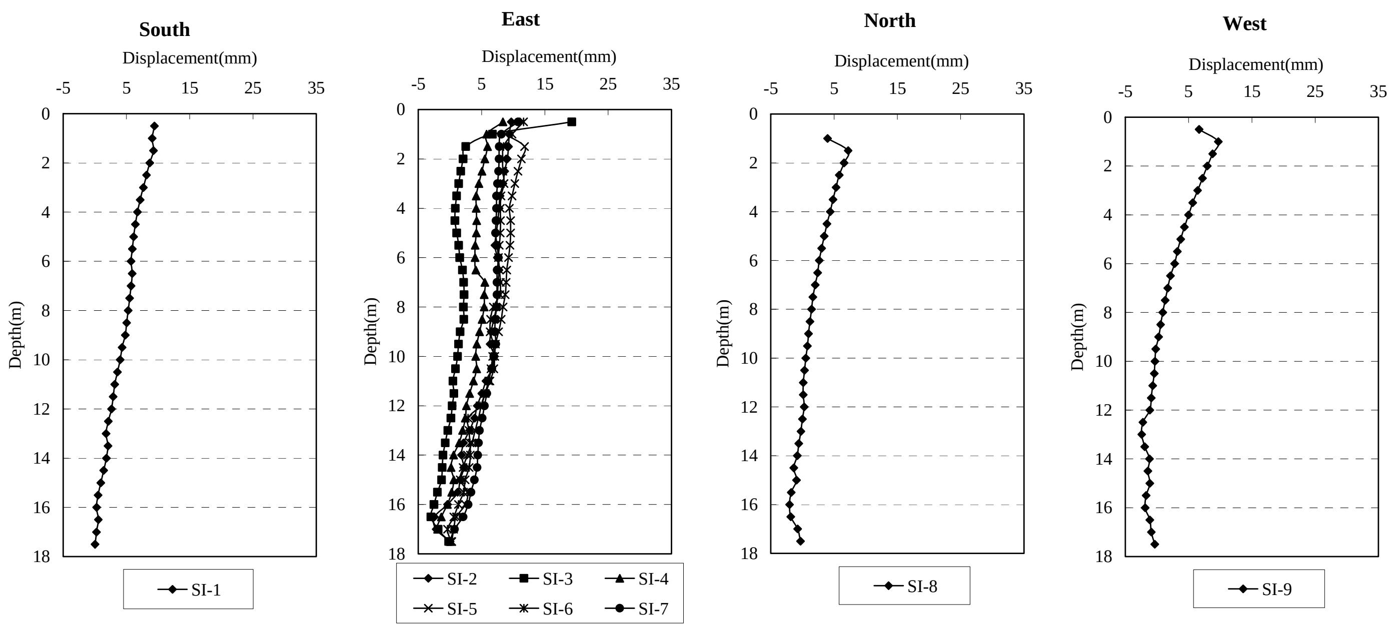

Fig. 13 Wall displacement curves (end of stage 2)

Table 5 Highest/lowest ground water levels recorded

Well number		OW-1	OW-2	OW-3	OW-4	OW-5	OW-6	OW-7	OW-8
Ground water level (m)	Highest	-6.05	-5.83	-5.52	-5.53	-5.23	-5.06	-5.23	-5.17
	Lowest	-8.38	-8.32	-9.07	-9.47	-9.18	-9.48	-9.05	-7.69
Well number		OW-9	OW-10	OW-11	OW-12	OW-13	OW-14	OW-15	OW-16
Ground water level (m)	Highest	-5.41	-5.20	-5.33	-5.25	-5.28	-5.04	-5.60	-5.29
	Lowest	-9.05	-8.95	-9.31	-8.56	-7.58	-7.49	-9.95	-8.94

water level is considered a representative drawdown as a consequence of the extensive dewatering within the project site. Roughly speaking, the ground water level dropped from GL.–4.9 m to GL.–8.3 m in the period of basement excavation, which was equivalent to an average drawdown of 3.4 m. The observed average drawdown was 1.4 m more than the expected 2 m as suggested by the local dewatering contractor, implying that the lateral pressure acting on the retaining side of the *T*-shaped wall was less than the design value.

Figures 14 and 15 are photos of the basement excavation at the end of Stage 2, revealing that the excavation itself and adjacent buildings were in stable condition.

9. DISCUSSION

The *T*-shaped diaphragm wall is modeled as a beam with an equivalent flexural stiffness in this paper, which is a conservative approach that mainly ignores the 3-D effect of *T*-shaped wall. As shown by the monitoring results, field performance of the *T*-shaped diaphragm wall was much less than expected. The maximum lateral displacement was controlled within 1.5 cm, and was found to occur at top of the wall. Shape of the field curve, which is characteristic of a cantilever beam, was in good agreement with the results calculated by RIDO. However, the maximum wall displacement observed in the field is only about 25% of the anticipated value, which can not be fully attributed to the high flexural stiffness of the *T*-shaped wall incorporated in the RIDO analyses. One simple explanation on the low displacement of *T*-shaped wall would be that the shear strength of the gravelly sand is much higher than anticipated. By comparing the results of parametric studies and field curves, it was easy to conclude that the "apparent" effective friction angle of the gravelly sand must exceed 35° to have a wall displacement less than 1.5 cm. An effective friction angle higher than 35° is unrealistic because the gravelly sand is loose to medium dense in nature. We believe the actual effective friction angle of the gravelly sand is about 32°±1°, therefore under estimating the shear strength of the gravelly sand is not a plausible scenario.

The authors postulate that side friction developed along the surface of buttresses provides additional passive resistance in limiting the lateral displacement of the *T*-shaped diaphragm wall (Fig. 16). Side frictions were generally mobilized at low strain level, which is difficult to be modeled in the RIDO analysis but do help in restricting the lateral wall displacement. *T*-shaped wall are often used as auxiliary measures to reduce diaphragm wall displacement in staged excavation (Hwang *et al*. 2007; Hsieh *et al*. 2008; Hwang and Moh 2008). In general practice, buttresses of the *T*-shaped wall are often demolished stage by stage, they are rarely used as the primary element of the excavation retaining system as outlined in this case history. Of course a 3-D numerical code can better model the *T*-shaped diaphragm wall. To what extent the side frictions helps in reducing wall displacement can perhaps be delineated by carrying out 3-D back analyses on the measured wall displacement, but it is obviously a task out of current scope.

Fig. 14 Completion of stage 2 excavation (south side, main entrance)

Fig. 15 Completion of stage 2 excavation (east side, adjacent buildings in the background)

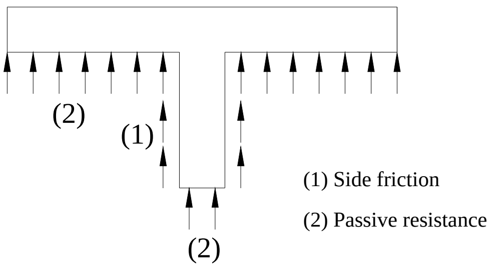

Fig. 16 Additional side frictions provided by the buttress of *T*-shaped wall

Another issue worth noting is the possible drawdown of ground water level behind *T*-shaped wall. The permeability of gravelly sand is so high that lowering the ground water level within the excavated side to GL.–10.6 m would definitely lead to drop of ground water level on the retaining side as a result of seepage. The designer was counting on the 18 m deep perimeter wall to provide a partial cutoff that could keep the dewatering induced ground settlement as low as possible, which seemed to be successful based upon the end result. The possible amount of drawdown can best be estimated by a 2-D or 3-D numerical tool, but once again, limited budget and time constraint had prohibited the designer to explore this issue further.

10. CONCLUSIONS

This paper demonstrated the successful use of *T*-shaped diaphragm wall as the retaining system of a large scale deep excavation project. Lateral displacement of the *T*-shaped diaphragm wall was kept within 1.5 cm when the intended excavation depth of 9.6 m was reached. Extensive pumping that involved the use of 200 deep wells was carried out to lower the ground water level 1m below the final excavation depth. The ground water table behind the *T*-shaped wall was lowered by an average of 3.4 m as a result of the extensive dewatering. The adjacent buildings suffered only minor non-structural damages due to settlement induced as a combined effect of excavation and dewatering.

Special care must be exercised on the construction of *T*-shaped diaphragm wall to ensure that the *T*-shaped wall is cast in one integral unit. The flexural stiffness of *T*-shaped wall is dramatically reduced if the perimeter wall and buttress wall are separately cast. Overlapping of the primary and secondary panels is also achieved by using a special joint that further increases the overall stiffness of the retaining system.

Simple beam-on-elastic foundation analyses were conducted to estimate the possible deformation of the *T*-shaped wall before excavation. It is obvious that this type of analysis is not able to fully capture the complex 3-D behavior of the *T*-shaped wall, but at least the results were on the conservative side. As a matter of fact, the 1-D analysis provided the designer with an intuitive view on the possible behavior of *T*-shaped wall, which is considered an advantage over the much complicated 3-D analysis. Field data did indicate that the designer over estimated the lateral displacement of the *T*-shaped wall, which can perhaps be attributed to the fact side frictions developed along the buttresses were not incorporated in the 1-D analyses.

Advanced analysis using robust 3-D numerical code is recommended to further study the behavior of *T*-shaped wall. The optimal length and depth of the buttress to support such kind of excavation are important design parameters that can be delineated by proper 3-D analyses. A proper 3-D analysis also provides a more realistic estimate on the lateral displacement of *T*-shaped wall, which is an essential number that must be kept low to maintain the integrity of adjacent buildings. The excavation scheme outlined in this paper using *T*-shaped wall as a main component of the retaining system can be implemented in future projects, provided that the behavior of *T*-shaped wall can accurately assessed by 3-D analysis in advance.

REFERENCES

Chang, J. J., Hsieh, M. D., and Wang, B. Y. (2001), "Assess of the excavation plan of a large-area foundation on gravelly sandy soil." *Sino-Geotechnics*, **85**, 43-50 (in Chinese).

Hsieh, H. S., Lu, Y. C., and Lin, T. M. (2008), "Effects of joint details on the behavior of cross walls." *Journal of GeoEngineering*, **3**(2), 55-60.

Hwang, R. N., Moh, Z. C., and Wang, C. H. (2007), "Performance of wall systems during excavation for core pacific city." *Journal of GeoEngineering*, **2**(2), 53-60.

Hwang, R. N. and Moh, Z. C. (2008), "Evaluating effectiveness of buttresses and cross walls by reference envelopes." *Journal of GeoEngineering*, **3**(1), 1-12.

Lee, K. H., Ou, C. D., and Tsai, K. W. (1992), "Quality control in construction of structural diaphragm wall joints." *Slurry Walls; Design*, Construction and Quality Control, Paul, D. B., Davidson, R. R., and Cavalli, N. J. Eds., ASTM STP-1129.

RIDO (1991), *User's Manual*, Version 3. Robert Fages Logiciels, France.

Woo, S. M. and Moh, Z. C. (1990), "Geotechnical characteristics of soils in the Taipei basin." *Proc. 10th Southeast Asian Geotech. Conf.,* Taipei, Taiwan, **2**, 51-65.

Xanthakos, P. P. (1994), Slurry Walls as Structural Systems, 2nd Ed., McGraw-Hill, Inc., New York, N.Y.